



## **BUCKLING BEHAVIOR OF LONGITUDINAL REINFORCING BARS IN CONCRETE COLUMN SUBJECTED TO REVERSE LATERAL LOADING**

**KUMIKO SUDA, YASUO MURAYAMA, TOSHIMICHI ICHINOMIYA, and HIROSHI SHIMBO**

Civil Engineering Department, Kajima Technical Research Institute  
Tobitakyu 2-19-1, Chofu-shi, Tokyo 182, JAPAN

### **ABSTRACT**

It is very important to predict accurately the load-displacement relationship of structural member for evaluating the earthquake resistance of large concrete bridges. Existing numerical models are, however, generally not capable of predicting the post peak behavior of the member. In this research, a series of tests of reinforced concrete (RC) column specimens were carried out focusing on the buckling of longitudinal reinforcing bars, which gives significant influence on the post peak behavior of RC column. In the tests, newly developed stress sensors, which measure stress in reinforcing steel bars after yielding, were used in order to find the change in stress of longitudinal reinforcing bars after buckling. Based on the test results, the buckling criteria and average stress-strain model of reinforcing bar after buckling are proposed.

### **KEYWORDS**

Reinforced Concrete, column, ductility, bridge pier, buckling, reinforcing bar, scaled model

### **INTRODUCTION**

Non-linear earthquake response analyses are performed in recent years in the seismic design of large prestressed concrete bridges for checking the safety of the structure against large earthquakes. Numerical models used for such an analysis is required to simulate the load-displacement relationships of structural members. Currently used models, however, cannot simulate well the softening phenomenon after reaching the ultimate bending moment in the structural member, because the effect of buckling of longitudinal reinforcing bars and that of spalling of cover concrete after the plasticization of the RC member are not reflected to the analyses. Many experimental researches have been carried out on the buckling of longitudinal reinforcing bars by uni-axial loading on the reinforcing bars themselves (Monti et al., 1992) or RC columns (Shima et al., 1990) for this reason. Reinforcement details with respect to longitudinal reinforcing bars and loading history of actual structures have not been taken into account. No method have been available until now for measuring the stresses in longitudinal reinforcing bars in a concrete member after yielding. This difficulty in measurement presents another reason why there has been little progress in

the research on this topic. Authors carried out a series of loading tests of RC column specimens in which newly developed stress sensors were used in order to find the buckling behavior of longitudinal reinforcing bars.

## STRESS SENSOR

Using a special heating coil (a coil of width 5 mm for a JIS D10 reinforcing steel bar), a very small area around the measuring position of the reinforcing bar was subjected to local induction hardening. A strain gauge was mounted at the center of the hardened part. The yield point of the measuring part was raised to more than 1.4 times that of the parent material (this assembly hereafter called stress sensor). Even if the parent material surrounding the stress sensor yields, the stress-strain relationship of hardened part remains linear because of raised yielding stress, therefore, the stress can be measured by reading the strain. As shown in Fig. 1, the range of thermal effects due to hardening extended approximately 1.5 times the diameter of the reinforcing bar, around the hardened part.

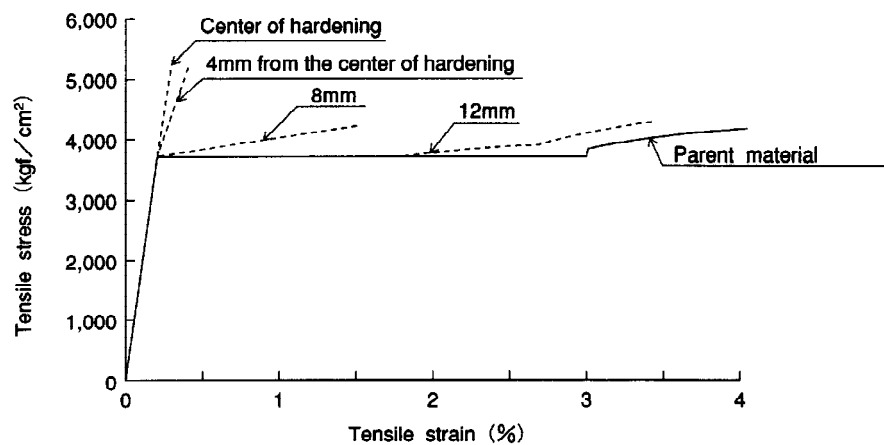


Fig. 1 Length of hardening

## OUTLINE OF TESTS

The parameters of specimens and properties of the materials are summarized in Table 1 and Table 2 respectively. Details of the specimens are illustrated in Fig. 2.

The relative displacements at the four corners of the cross section at 450mm (1.5 times the depth of the cross section) above the footing surface were measured. From these measured values, the average curvature and the average strain at each corner in the cross section were determined.

Table 1 Specimens and loading

Specimen No.	Longitudinal reinforcement		Transverse reinforcement			Shear span ratio	Axial stress (kgf/cm <sup>2</sup> )
	Diameter	ratio (%)	Diameter	Spacing (mm)	ratio (%)		
1	D10	2.6	Deformed 3mm dia.	45	0.16	10	62
2			Deformed 4mm dia.		0.28		
3				80	0.16	5	13
4			Deformed 3mm dia.	45			

Table2 Properties of specimens

Concrete	Specimen No.	Compressive strength (kgf/cm <sup>2</sup> )	Elastic modulus (kgf/cm <sup>2</sup> )
	1	438	$3.0 \times 10^5$
	2	457	$3.0 \times 10^5$
	3	462	$3.3 \times 10^5$
	4	459	$3.1 \times 10^5$
Reinforcement	Diameter	Yield stress (kgf/cm <sup>2</sup> )	Tensile strength (kgf/cm <sup>2</sup> )
	D10	3,590	5,340
	Deformed 3mm dia.	3,790	4,900
	Deformed 4mm dia.	3,050	4,350

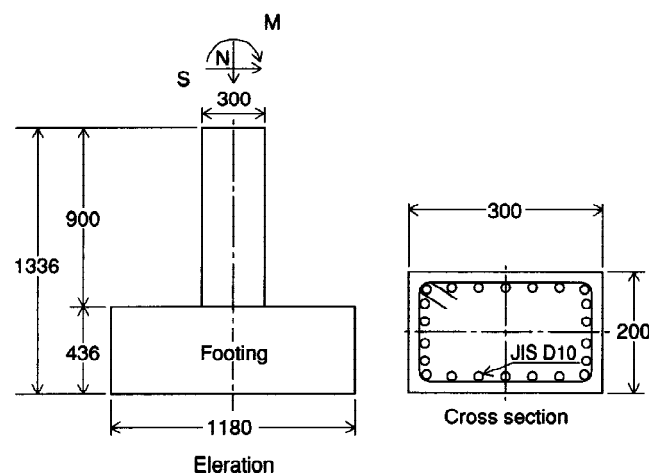


Fig. 2 Details of specimens

The stress sensors and conventional strain gauges were installed on two sides in the axial direction of the longitudinal reinforcing bars to obtain average axial stress and average axial strain. The stress sensors and the conventional strain gauges were mounted at two vertical location of the two centrally positioned reinforcing bars, on the footing surface and 9 cm above (for stress sensor only).

## LOADING METHOD

Load was applied on the head of the RC column using a loading apparatus capable of applying an arbitrary combination of forces. Bending moment and shear force (refer to Table 1 for shear span ratio) were applied in the reversed and cyclic manner. The axial compressive stress was retained at 62kgf/cm<sup>2</sup> for towers, and 13kgf/cm<sup>2</sup> for piers.

Load was controlled before the yielding of the column, while deformation was controlled after the yielding based on  $n$  times the average curvature at yield point (in 450-mm measuring range), where  $n$  is an integer.

## TEST RESULTS

As shown in Fig. 3 a), the cover concrete at the base of the column split at maximum load. Subsequently, during cyclic loading, the cover concrete spalled and the longitudinal reinforcing bars buckled, leading to a

failure of the column. The failure process was almost similar for all of the specimens.

As shown by the circular black mark “●” mark in Fig. 3 c), a kink point from rise to drop in the compressive stress is observed in spite of the continuous application of bending moment. The black mark position is defined as the point at which buckling starts. The corresponding point is also shown in Fig. 3 a), b) and d).

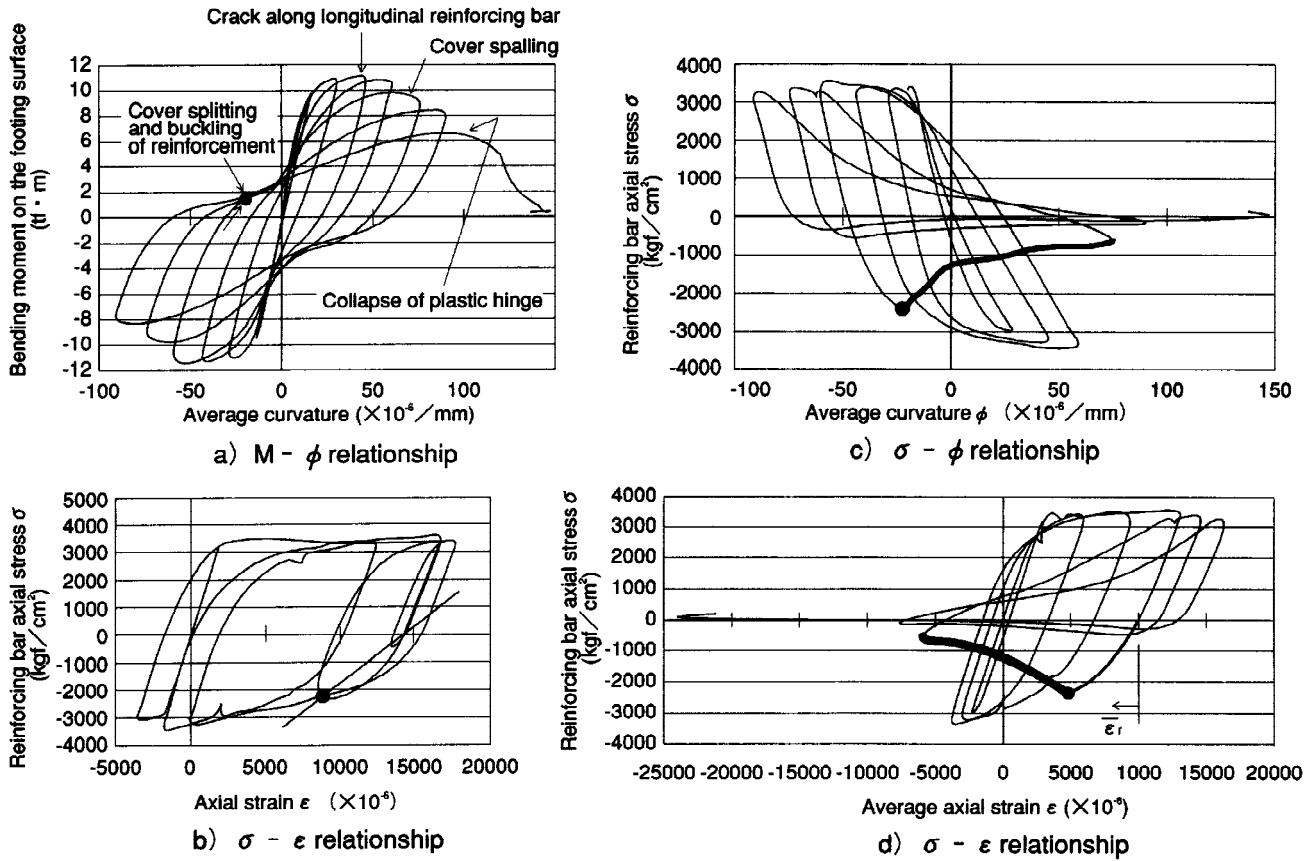


Fig. 3 Examples of Test Results (No.1 specimen)

As shown in Fig. 3 d), the relationship between the axial stress and the axial strain in the reinforcing bar indicates hysteresis characteristics similar to the test results of a steel bar by Monti et al., (1992). Buckling, however, occurs at a point in the tensile strain region before the compressive strain is applied. The curvature of the member due to flexural deformation significantly influences when buckling starts in the reinforcing bars. The compressive stress does not come back to zero immediately after buckling, but gentle softening characteristics are rather exhibited. When tension is reapplied in the next cycle, the tensile stress in the strain level equal to the maximum strain in the previous cycle becomes smaller.

Once the reinforcing bar buckles, it does not take up almost any stress in the following compressive loading stage. The compressive stress reduces to 10%-20% of the buckling stress.

## DISCUSSION OF TEST RESULTS

The followings are the factors influencing the buckling behavior of reinforcing bars in the RC column when many longitudinal reinforcing bars were arranged on each side of the cross section:

a) splitting strength of concrete near the longitudinal reinforcing bars



- b) flexural stiffness of transverse reinforcing bars
  - c) flexural stiffness of the longitudinal reinforcing bars
- The influences of these factors are discussed in the following.

#### *Comparison with Elastic Buckling Theory*

Buckling load of the longitudinal reinforcing bar was calculated with elastic theory. A beam, which is fixed at both ends and elastically supported, was assumed to represent a longitudinal reinforcing bar. A semi-circular buckling mode was considered. The elastic modulus of the bar was given as the secant modulus of zero-stress point to the point where buckling starts (Fig. 3 c). The elastic spring constant was evaluated from the flexural stiffness of transverse reinforcing bars, which was assumed to be fixed at both ends.

Computed buckling stress in the longitudinal reinforcing bar is compared with the measurement in Fig. 4, which shows the smaller theoretical values. The similar results were obtained for the other specimens. Since the longitudinal reinforcing bar has a certain curvature due to the residual deformation, when the buckling occurs, the buckling load by a method considering the deformation is thought to be even smaller than the value by the present method which assumes no deformation. This is verified by FEM analysis.

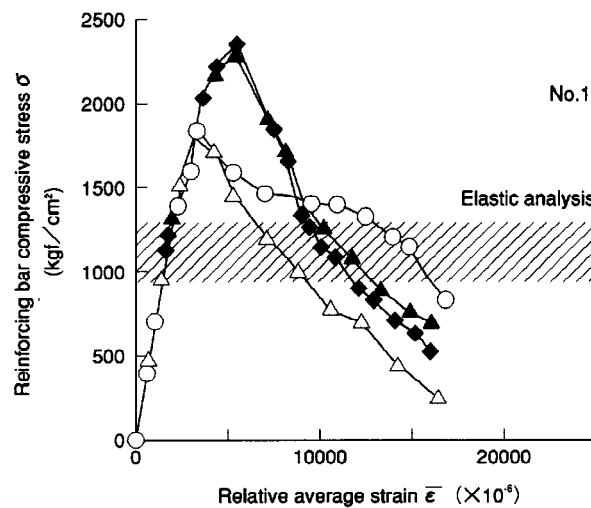


Fig. 4 Buckling Stress

In actual structure, the diameter of reinforcing bar is smaller compared to the dimensions of cross section, which implies that the effect of flexural stiffness of longitudinal and transverse reinforcing bars on buckling is smaller than that in model specimen. These facts suggest that the influence of a) is more significant on the buckling of the reinforcing bar than the influence of b) and c).

#### *Splitting Strength of Cover Concrete*

Compressive force applied on a longitudinal reinforcing bar with a certain degree of curvature, as shown in Fig. 5, generates a force  $\Delta H$  that tries to push the cover concrete outward. The amount of  $\Delta H$  is proportional to the product of the stress and the curvature. According to the observed data, this product took a maximum value near the point in the loading history where buckling starts. Fig. 6 shows the relationship between the splitting stress due to  $\Delta H$  at the buckling and the maximum compressive strain of the cover concrete before the buckling. This figure also includes the data by Maekawa et al. (1983) and Liners (1987). It is found that the buckling of a longitudinal reinforcing bar is dependent upon the splitting strength of the cover concrete even if it is extremely small.

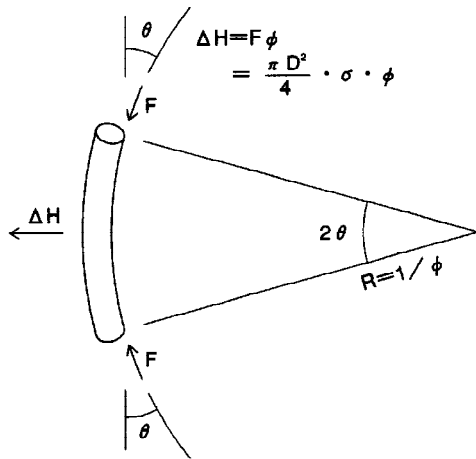


Fig. 5 Horizontal force by Reinforcing Bar

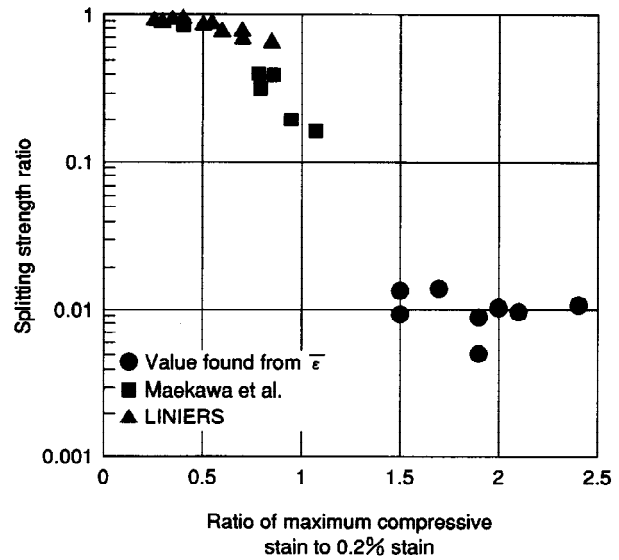


Fig. 6 Splitting Strength of Cover Concrete

### Hysteresis Characteristics of Longitudinal Reinforcing Bar after Buckling

Fig. 7 shows the relationship between measured average axial stress and measured average axial strain in the longitudinal reinforcing bar, which corresponds to the softening curve (the bold line) shown in Fig. 3 d. In this figure, the compressive stress is normalized with the buckling stress, while the strain represents the change from the strain at the onset of buckling. As observed in the figure, although there is variation in the measured data, the slope after the onset of buckling for each case is almost the same. If the curve is extrapolated to intersect the horizontal axis, the change in strain from buckling point is approximately 1.8 to 2.0%.

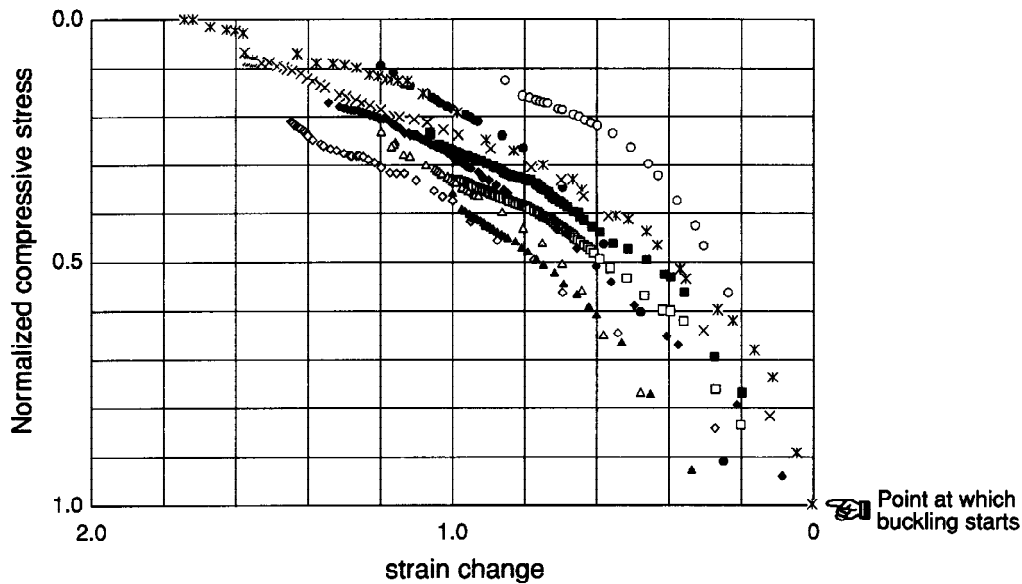


Fig. 7 Softening Curve after Buckling

Fig. 8 shows the relationship between the ratio of the reapplied tensile stress to the maximum tensile stress just before buckling ( $\sigma_{t1}/\sigma_{t0}$ ) and the change of compressive strain after buckling. For the change in strain of less than approximately 1%, the reapplied stress is almost equal to  $\sigma_{t0}$ . However, if the change in strain exceeds 1%, the tensile stress decreases with the change in strain. When the change in strain reaches at 2%, the stress decreases to approximately 90% of the stress before buckling.

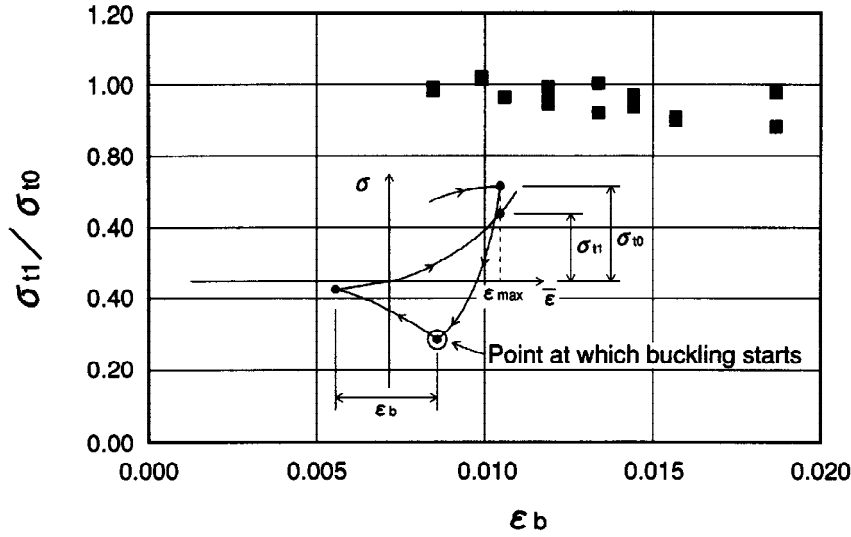


Fig. 8 Stress at re-application of tension after buckling

## BUCKLING MODEL

### *Method of Determining the Point at which Buckling Starts*

In the actual structure, the effect of the flexural stiffness of the longitudinal reinforcing bar and the constraints by transverse reinforcing bars are considered to be small. Consequently, the effect of cover concrete on buckling becomes dominant. To determine the point at which buckling starts, a horizontal force  $\Delta H$ , which is expressed as a function of the product of stress in the reinforcing bar and curvature of the member, was assumed to be equivalent to the total splitting force acting on the cover concrete. The splitting strength of the cover concrete is estimated from the maximum compressive strain experienced at the position of the longitudinal reinforcing bar. The stress-strain relationship in the reinforcing bar after this point is assumed to follow the hysteresis model described below.

### *Modeling the Stress-Strain Relationship after Buckling*

The average stress-strain relationship after buckling is modeled as shown in Fig. 9. Point B, where buckling starts, is determined according to the method described above. The path for compressive softening after buckling and the path where the longitudinal reinforcing bar is subjected to a tensile stress, are modeled by straight lines, BC and CE, respectively. Point P, (obtained by extrapolation of BC) is defined by the change in strain from the onset of buckling towards compression, which is given by  $\epsilon_{b0} = 2\%$ . Point D, through which the line CE passes, is taken as the position of maximum tensile strain in the previous cycle, and the corresponding tensile stress  $\sigma_{t,i}$ , where  $i$  is the number of loading times after buckling, is defined by the following equation:

$$\sigma_{t,i} = \sigma_{t,i-1} \times \alpha(\epsilon_b)$$

where,

$$\alpha(\epsilon_b) = \begin{cases} 1.0 & (\epsilon_b \leq 1\%) \\ 1.1 - 0.1 \epsilon_b & (\epsilon_b > 1\%) \end{cases} \quad (\epsilon_b \text{ unit ; percent})$$

EF and FG follow the conventional hysteresis model. The compressive stress at point G is taken as 10% of the stress at point B. Point P is taken as the target for all stages during compressive softening.

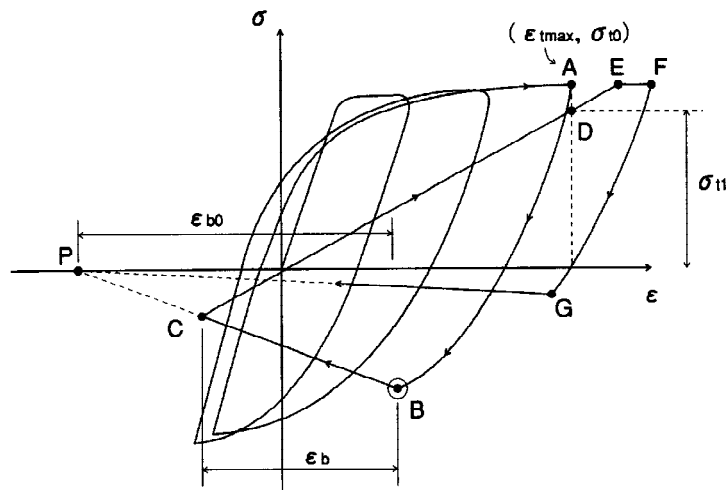


Fig. 9 Hysteresis Model after Buckling

## CONCLUSION

The buckling behavior of longitudinal reinforcing bars in RC columns was studied experimentally. The following conclusions are obtained:

- 1) The relationship between average axial stress and average axial strain in a longitudinal reinforcing bar after buckling was clarified by the model tests.
- 2) The relationship between average axial stress and average strain in a longitudinal reinforcing bar in RC column after buckling differs from the test results of steel bar alone. Buckling occurs at a comparatively small compressive stress in a reinforcing bar with residual tensile strain.
- 3) In RC members such as towers and piers, the flexural stiffness of the reinforcing bar itself, and constraints due to transverse reinforcing bars have only minimal effect on the buckling of the longitudinal reinforcing. On the other hand, the constraining effect of the cover concrete on the buckling is significant.
- 4) A buckling model of longitudinal reinforcing bars that includes all of the characteristics mentioned above is proposed.

## REFERENCES

- Liners, D.(1987). Micro cracking of Concrete under Compression and its Influence on Tensile Strength, *Materials and Structures*, **20**,111-116.
- Maekawa, Koichi et.al.(1983). Deformation Behavior of Concrete Under Biaxial Compression-Tension Stress State, *Concrete Journal*, Japan Concrete Institute, **21**, No. 3, 111-121.
- Monti, G. et.al.(1992). Nonlinear Cyclic Behavior of Reinforcing Bars Including Buckling, *Journal of Structural Engineering*, ASCE, Vol. 118, **12**, 3268-3284.
- Shima, Hiroshi et.al. (1990). Ductility Analysis Using Reinforcement Buckling Model of RC Bridge Piers Subject to Reverse Loading, *Proceedings of Japan Concrete Institute* ,**12**,741-746.